Self-Assembled Magnetic Surface Swimmers

A. Snezhko,[1] M. Belkin,[1,2] I. S. Aranson,[1] and W.-K. Kwok[1]

[1]*Materials Science Division, Argonne National Laboratory, 9700 South Cass Avenue, Argonne, Illinois 60439, USA*
[2]*Illinois Institute of Technology, 3101 South Dearborn Street, Chicago, Illinois 60616, USA*

(Received 14 October 2008; published 16 March 2009)

We report studies of novel self-assembled magnetic surface swimmers (magnetic snakes) formed from a dispersion of magnetic microparticles at a liquid-air interface and energized by an alternating magnetic field. We show that under certain conditions the snakes spontaneously break the symmetry of surface flows and turn into self-propelled objects. Parameters of the driving magnetic field tune the propulsion velocity of these snakelike swimmers. We find that the symmetry of the surface flows can also be broken in a controlled fashion by attaching a large bead to a magnetic snake (bead-snake hybrid), transforming it into a self-locomoting entity. The observed phenomena have been successfully described by a phenomenological model based on the amplitude equation for surface waves coupled to a large-scale hydrodynamic mean flow equation.

DOI: 10.1103/PhysRevLett.102.118103 PACS numbers: 87.19.ru, 47.63.Gd, 75.50.Tt

Fundamental mechanisms governing locomotion at the macro- and microscale are attracting enormous attention in the physics community [1–10]. The interest is driven by the need for understanding how biological organisms propel themselves in various environments and by the growing demand for the design of artificial externally controlled structures capable of performing useful tasks at the microscale, including targeted cargo delivery [11,12] or stirring in microfluidic devices [13]. Several concepts of low-Reynolds number microswimmers were proposed, including three-sphere swimmers [3] and magnetic swimmers based on DNA-linked colloidal magnetic particles [5]. Typically, the propulsion mechanism is associated with a breaking of the time-reversal symmetry of the reciprocal motion of the swimmer's body [14], such as rotation of helical flagella of motile bacteria.

In our earlier studies [15,16] we reported the self-assembly of magnetic microstructures (magnetic snakes) in a dispersion of magnetic microparticles suspended at a water-air interface and subjected to a vertical alternating magnetic field. These structures appear due to the coupling between surface deformations of the fluid and the collective response of particles to an external alternating magnetic field. In the course of the alignment of the particle's magnetic moment with the external field, the particles produce local deformations of the water surface, thereby affecting neighboring particles. These deformations bring particles close enough that the head-to-tail dipole-dipole attraction overcomes the repulsion caused by the external field. As a result, chains of particles are formed with resulting magnetic moments pointing along the chains. The chains produce wavelike local motion facilitating the self-assembly process (the component of the magnetic field parallel to the surface of the water further promotes the chain formation, see Ref. [16] for detail). Magnetic snakes consist of sections (segments) formed by ferromagnetically aligned chains of microparticles. The length of the segments is defined by the wavelength of the surface wave (two segments per wavelength). Segments, however, are always antiferromagnetically ordered [17–19].

In this Letter we report the discovery of a novel type of self-assembled magnetic surface swimmers that form in the same system, magnetic microparticles at a water-air interface. We find that under certain conditions magnetic snakes spontaneously break the symmetry of surface flows and turn into self-propelled entities. Alternatively, another type of swimmers is realized via controlled breaking of the symmetry of surface flows by attaching a bead to one of the snake's ends (bead-snake hybrid). Both types of magnetic swimmers are unique due to the unusual mechanism of self-propulsion exploiting symmetry breaking of self-generated surface flows and the intrinsic antiferromagentic nature of the swimmer's structure. The magnetic field parameters can be used to control the propulsion velocity and the structure of the swimmers. Our phenomenological model successfully reproduces observed experimental observations.

Our experimental setup is similar to that reported in [15], however with a number of modifications: more than a fourfold increase in the area of experimental cell and in the bore of the coils, and considerably increased values of accessible magnetic fields. A glass beaker (10 cm in diameter) is filled with water and placed in the center of precision Helmholtz coils (13 cm in diameter) capable of creating vertical magnetic fields up to 170 Oe. Magnetic microparticles (90 μm Nickel spheres) are suspended at the surface of water and supported by surface tension. The positions of the particles are monitored by a high-speed camera mounted on an optical microscope stage. A homogeneous vertical sinusoidal magnetic field $\mathbf{H} = H_0 \sin(2\pi f t)\mathbf{z}_0$ with amplitude H_0 and frequency f was applied.

The snake is accompanied by four large symmetric hydrodynamic vortices located at the opposite ends of the snake [17] (vortex quadrupole). As a result, two ends of the snake represent miniature engines pumping surrounding liquid in opposite directions. Figure 1(a) shows the flow created by one of such ''engines'' obtained by particle image velocimetry (PIV). The flow generated by the snake could be as fast as a few centimeters per second and is controlled by the frequency and amplitude of the external magnetic field [17]. In a low frequency case (frequency of the external magnetic field is below about 100 Hz), both ''engines'' are identical. Consequently, the flows are exactly compensated and the snake is at rest (no translational movement in the x-y plane). However, we have found that as the frequency of the magnetic field is increased, a stationary snake transforms into a self-propelled magnetic swimmer via spontaneous symmetry breaking of the balance between the engines, and, consequently, of the quadrupole vortex structure. The experimental observation of this behavior is illustrated in Fig. 1(b) and movies 1 and 2 [18]. There is no sharp transition frequency but a transition region, about 30 Hz wide at around 100 Hz. Once transformed into a self-propelled swimmer, the snake tends to swim on a straight line unless it collides with the wall of the container or other snake. Collisions with the wall typically lead to a subsequent destruction of the snake and reassembly of another snake at a different location. Depending on the initial density of magnetic particles at the surface of the liquid, more than one self-propelled snake may appear at the same time (the higher the density, the more snakes could be induced), see movie 2 [18]. In the case of multiple swimmers, their shape, length, and sometimes even the total number of snakes may vary. A closer look at the mechanism of self-propulsion of an initially motionless snake reveals a drastic spontaneous change of its flow pattern. Figure 1(c) shows the surface flow structure of a swimming snake. Apparently, as the frequency of the magnetic field is increased, the snake develops a highly asymmetric vortex structure. One pair of vortices associated with one of the snake's tails becomes stronger than another, meaning that one of the engines becomes more powerful. The resulting net difference in the power of the engines propels the snake.

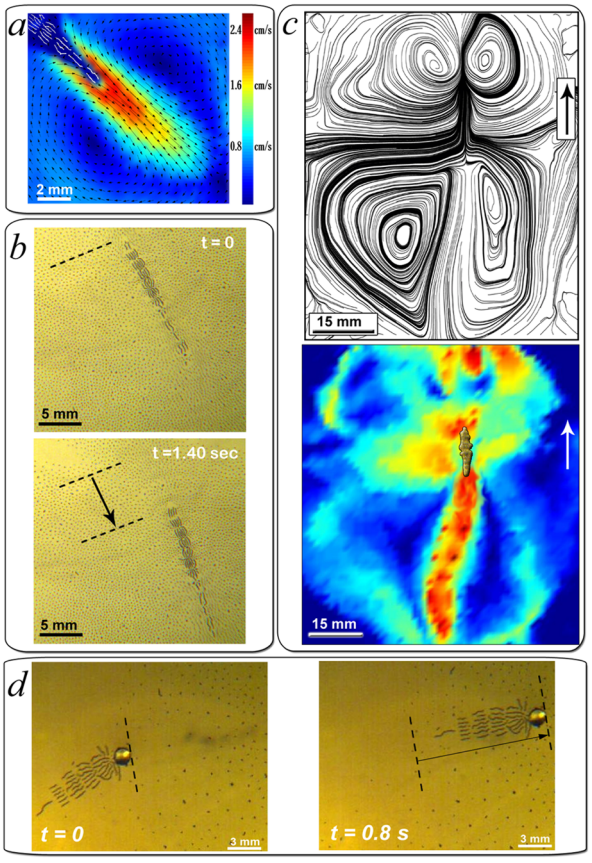

FIG. 1 (color online). Magnetic swimmers generated by a vertical alternating magnetic field. (a) Surface flow velocity field in the vicinity of the snake's tail. Arrows depict the surface velocity field obtained by PIV and the background colors show relative magnitudes of flow velocities. (b) Self-propelled magnetic swimmer energized by a 100 Oe, 140 Hz vertical magnetic field. (c) The vortex structure of a self-propelled snake. Arrow shows the direction of swimming. The bottom image illustrates the amplitude of surface flows around the swimming snake. Dark blue (dark gray) color corresponds to low velocities of flows; a long jet stream emanates from one of the snake's tails. (d) Self-propelled snake-particle hybrid, $f = 80$ Hz, $H_0 = 100$ Oe, 1.5 mm spherical glass bead is used.

The bottom image of Fig. 1(c) displays the amplitude of the flow velocity in the vicinity of the magnetic swimmer: a long jet stream emanating from one of the snake's tails reveals the uncompensated flow generated by the swimmer. In our experiments, self-propelled snakes appear at random locations and then swim on straight trajectories in the direction determined by their initial orientations, see movie 2 [18]. Whereas the velocity of the snakes can be tuned by parameters of the external magnetic field (higher frequencies produce more rapid swimmers), their propulsion direction could not be easily controlled by the external magnetic field in contrast to artificial magnetic swimmers assembled from DNA-linked magnetic microparticles [5]. While in the latter case the swimmer simply moves along a static in-plane magnetic field, self-propelled snakes react completely different to external in-plane fields due to their intrinsic antiferromagnetic nature [15,16,19] resulting in a zero net magnetic moment of the structure.

We have found experimentally that it is also possible to create a self-propelled magnetic swimmer from a stationary snake even below the threshold of self-propulsion instability. It can be done by placing a large glass or polystyrene bead (1–2 mm) near one of the snake's tails. The snake often self-attaches to the bead forming a stable swimming bead-snake hybrid. This bead suppresses the vortex flow at one of the snake's tails giving rise to uncompensated flow that propels the swimmer (see movie 3 [18]). Figure 1(d) shows a sequence of snapshots illustrating the motion of the structure with a 1.5 mm spherical glass bead. In our experimental setup we were able to

create such stable snake-particle hybrids moving in circles along the container wall (see movies 4 and 5 [18]).

Figure 2 shows the swimming velocity of the snake-particle hybrid vs external magnetic field amplitude. The velocity closely follows a quadratic dependence on the external field amplitude H as one would anticipate for a streaming flow induced by an oscillating object (compare to Rayleigh streaming) [20], $V \sim fA^2/a_0$, where A is the amplitude of vertical oscillations of the tail which is proportional to amplitude of the magnetic field H, and a_0 is the typical size of a snake segment (of the order of the wavelength λ). We find that the swimming velocity is of the same order as the velocity of the stream generated by a stationary snake (see insert to Fig. 2).

To obtain insights into the mechanism of self-propulsion, we extended the phenomenological model reported in Ref. [17]. This model is formulated in terms of a paradigm Ginzburg-Landau type equation for parametric surface waves coupled to the conservation law for the magnetic particle density and the equation for large-scale mean flow. To describe the mechanism of spontaneous symmetry breaking of the surface flow structure and formation of self-propelled swimmers, the last two terms in Eq. (1) have been introduced into the model [Eqs. (1)–(3)].

$$\partial_t \psi + (\mathbf{v}\nabla)\psi = -(1 - i\omega)\psi + (\varepsilon + ib)\nabla^2\psi - |\psi|^2\psi + \gamma\psi^*\phi(\rho) + i\alpha_1\psi^*(\nabla\psi)^2 - i\alpha_2\psi|\nabla\psi|^2 \quad (1)$$

$$\partial_t \rho + \nabla(\rho\mathbf{v}) = D\nabla^2\rho - \beta\nabla(\rho\nabla|\psi|^2) \quad (2)$$

$$\partial_t \mathbf{v} + (\mathbf{v}\nabla)\mathbf{v} + \frac{\nabla p}{\rho_f} = \nu\nabla^2\mathbf{v} + \mathbf{F} \quad (3)$$

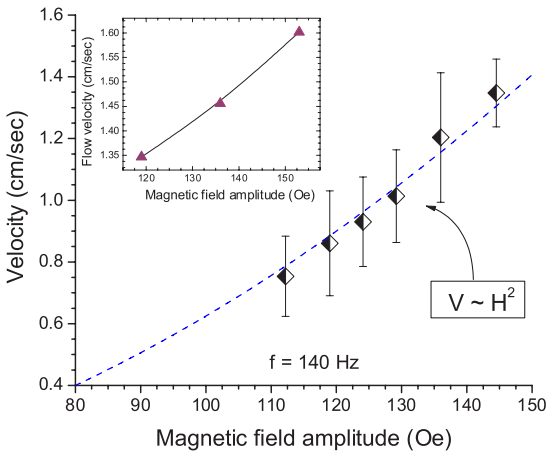

FIG. 2 (color online). Mean swimming velocity of the snake-bead hybrid vs amplitude of the magnetic field at $f = 140$ Hz. The dashed line is a fit to quadratic dependence of the swimmer velocity on the amplitude of the external field, $V \sim H^2$. Insert: flow velocity at the tail of the stable snake generated at $f = 140$ Hz. The swimming velocity is of the same order as the maximum flow velocity of a stationary snake.

In Eq. (1) the field ψ describes the complex amplitude of surface waves. Forcing by the external alternating magnetic field (parametric driving) is described by the term $\gamma\psi^*\phi(\rho)$, terms $|\psi|^2\psi$ and $\varepsilon\nabla^2\psi$ account for nonlinear damping and viscous dissipation (see [21] for detail). Function $\phi(\rho)$ in the driving term accounts for the saturation of forcing at higher values of particle density ρ. The conservation law for the magnetic particles' density ρ is represented by Eq. (2), where D is the diffusion coefficient, and the advection term (which describes advection of particles by waves) has the amplitude β. Equation (3) is a Navier-Stokes equation for the evolution of the large-scale hydrodynamic velocity field $\mathbf{v}$. p is the pressure and ρ_f and ν are the fluid's density and viscosity, respectively. We assume that the characteristic scale of the hydrodynamic field $\mathbf{v}$ is much larger than that associated with surface waves. It allows consideration of the situation when the large-scale flow $\mathbf{v}$ is purely two-dimensional that leads to a considerable simplification of Eq. (3) by introducing a stream function Ω, $v_x = \partial_y\Omega$, $v_y = -\partial_x\Omega$. The external driving, averaged over one period, is taken into account by the vector force $\mathbf{F}$, whose form, for the symmetry reasons, is chosen to be $\mathbf{F} = \zeta(\psi^*\nabla\psi - \psi\nabla\psi^*)$. The last two terms in Eq. (1) are formally higher order compared to other terms (in the framework of the Ginzburg-Landau theory). Our simulations revealed that these two terms are responsible at least for two nontrivial effects. (i) They provide structural rigidity of the snake and control its length to width ratio. Without these terms the snake appears to be compressed by flows generated from the tails (segments in the center become much wider than at the tails). (ii) For large enough magnitude of $\alpha_{1,2}$ the snake exhibits a symmetry-breaking instability and onset of spontaneous swimming similar to that observed in the experiment.

Figure 3 shows the numerical solution of Eqs. (1)–(3). The model captures the onset of symmetry-breaking instability of the quadrupole vortex structure when the snake develops spontaneous swimming (see also movie 6 [18]). The inset in Fig. 3 displays the stream function of the moving snake as obtained from simulations. One sees a profound asymmetry of surface vortex flows developed by the snake. The swimming velocity exhibits a square root dependence on the external driving γ, the hallmark of the symmetry-breaking instability (solid line in Fig. 3).

Our model has also successfully captured a translational motion of the snake when flows were intentionally suppressed at one of the snake's ends (see movie 7 [18]). In order to perform simulations of a snake-bead hybrid, we modeled the influence of the spherical bead by introduction of an attenuation of the forcing term, $\mathbf{F}$, in the vicinity of one of the snake's tails. A typical flow structure in the vicinity of the snake-particle hybrid, as obtained from the simulations, is shown in Fig. 4.

To conclude, we have found a new realization of self-assembled magnetic swimmers. Being self-assembled

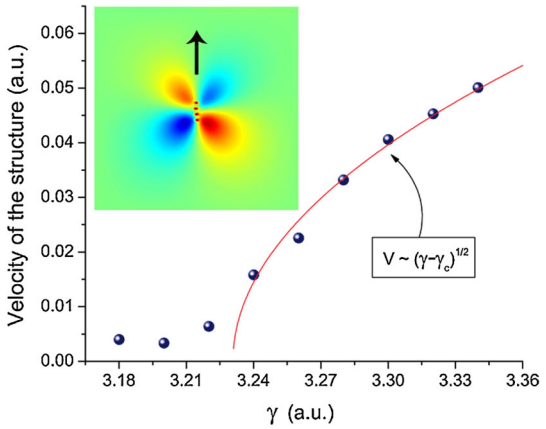

FIG. 3 (color online). Numerical studies of a self-propelled snake showing the onset of the snake's symmetry breaking and swimming. The solid line is a fit to a $(\gamma - \gamma_c)^{1/2}$ dependence. Inset: spontaneous symmetry breaking of the snake's quadrupole vortex flows (colors represent the values of the stream function Ω) obtained from Eqs. (1)–(3). Arrow shows the direction of swimming, note the asymmetry between vortex pairs. Parameters in Eqs. (1)–(3) are: $\varepsilon = 1$, $b = 5$, $\gamma = 3.32$, $D = 0.2$, $\beta = 60$, $\omega = 3$, $\alpha_1 = 100$, $\alpha_2 = 500$, $\nu = 1.5$, $\zeta = -7$ in a domain of water-air 200×200 dimensionless units.

from a dispersion of magnetic particles in a system with complex (magnetic, hydrodynamic) interactions, the swimmers have the ability to exhibit propulsion due to spontaneous breaking of the symmetry of quadrupole vortex flows. We show that self-assembled magnetic swimmers can also be realized by the controlled breaking of the flow symmetry leading to stable snake-bead hybrids. Our results yield fundamental insights into mechanisms of self-assembly and locomotion in nonequilibrium systems with complex interactions between particles, and also provide an interesting opportunity to model surface locomotion of living organisms [22]. One of the immediate applications of these novel swimmers may be their use as effective surface mixers to stir components at the liquid-gas interface. Snake-bead hybrids also open a new intriguing opportunity for functionalization of the snake's head for the purpose of targeted delivery or transport where the control over the swimmer's direction may be gained through use of spatially inhomogeneous fields.

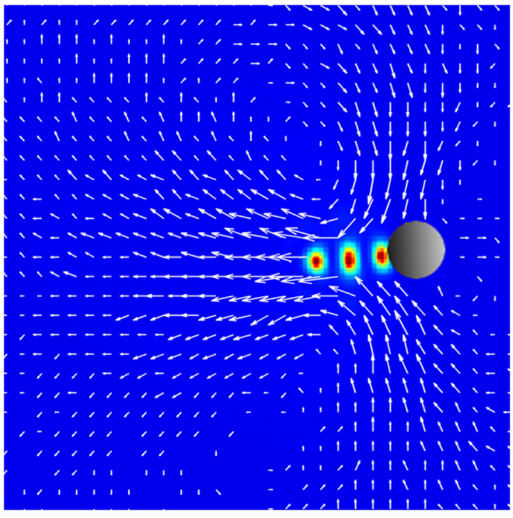

FIG. 4 (color online). Velocity field of a snake-particle hybrid (arrows), colors show the value of $|\psi|^2$. The simulation is performed at $\omega = 2.95$, $\gamma = 3.20$. The gray circle in the image depicts the area where the forcing term $\mathbf{F}$ in Eq. (3) is suppressed.

This research was supported by US DOE, Grant No. DE-AC02-06CH11357.

[1] J. E. Avron, O. Gat, and O. Kenneth, Phys. Rev. Lett. **93**, 186001 (2004).
[2] R. Golestanian and A. Ajdari, Phys. Rev. Lett. **100**, 038101 (2008).
[3] A. Najafi and R. Golestanian, Phys. Rev. E **69**, 062901 (2004).
[4] C. M. Pooley and A. C. Balazs, Phys. Rev. E **76**, 016308 (2007).
[5] R. Dreyfus *et al.*, Nature (London) **437**, 862 (2005).
[6] F. Y. Ogrin, P. G. Petrov, and C. P. Winlove, Phys. Rev. Lett. **100**, 218102 (2008).
[7] D. C. Rapaport, Phys. Rev. Lett. **99**, 238101 (2007).
[8] J. E. Avron and O. Raz, New J. Phys. **10**, 063016 (2008).
[9] A. M. Leshansky and O. Kenneth, Phys. Fluids **20**, 063104 (2008).
[10] R. Trouilloud, T. S. Yu, A. E. Hosoi, and E. Lauga, Phys. Rev. Lett. **101**, 048102 (2008).
[11] J. Edd *et al.*, in Proceedings of the IEEE/RSJ. Intl. Conf. on Intelligent Robots and Systems (IEEE, New York, 2003), Vol. 3, pp. 2583–2588.
[12] O. Raz and A. M. Leshansky, Phys. Rev. E **77**, 055305(R) (2008).
[13] S. T. Chang *et al.*, Nature Mater. **6**, 235 (2007).
[14] E. M. Purcell, Am. J. Phys. **45**, 3 (1977).
[15] A. Snezhko, I. S. Aranson, and W.-K. Kwok, Phys. Rev. Lett. **96**, 078701 (2006).
[16] A. Snezhko, I. S. Aranson, and W.-K. Kwok, Phys. Rev. E **73**, 041306 (2006).
[17] M. Belkin, A. Snezhko, I. S. Aranson, and W.-K. Kwok, Phys. Rev. Lett. **99**, 158301 (2007).
[18] See EPAPS Document No. E-PRLTAO-102-045912 and ANL website http://mti.msd.anl.gov/highlights/snakes/ for movies illustrating dynamic self-assembled magnetic swimmers. For more information on EPAPS, see http://www.aip.org/pubservs/epaps.html.
[19] A. Snezhko and I. S. Aranson, Phys. Lett. A **363**, 337 (2007).
[20] N. Riley, Q. J. Mech. Appl. Math. **19**, 461 (1966); M. Belovs and A. Cebers, Phys. Rev. E **73**, 051503 (2006).
[21] I. S. Aranson and L. S. Tsimring, Rev. Mod. Phys. **78**, 641 (2006).
[22] J. W. M. Bush and D. L. Hu, Annu. Rev. Fluid Mech. **38**, 339 (2006).